Analyst

Accepted Manuscript

ROYAL SOCIETY OF CHEMISTRY

www.rsc.org/analyst

Table of Contents

A frequency at the susceptance minimum (f_{Bmin}) is applied to assess the kinetics of RXRα to specific and non-specific oligoduplexes.

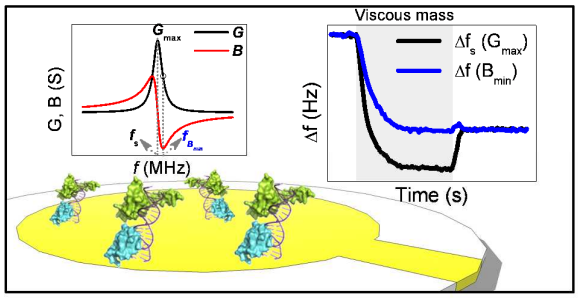

Analyst

RSCPublishing

ARTICLE

Kinetic characterization of retinoic X receptor binding to specific and unspecific DNA oligoduplexes with quartz crystal microbalance

R.M.M. Rodrigues,[a] J. de-Carvalho[a] and G. N.M. Ferreira[a,b]

Cite this: DOI: 10.1039/x0xx00000x

Received 00th January 2012,
Accepted 00th January 2012

DOI: 10.1039/x0xx00000x

www.rsc.org/

Quartz Crystal Microbalance (QCM) biosensor technology was used to study the interaction of the DNA-binding domain (DBD) of the transcription factor RXRα with immobilized specific (DR1) and unspecific ($DR1_{neg}$) DNA oligoduplexes. We identify the QCM sensor frequency at the susceptance minimum (f_{Bmin}) as a better measuring parameter, and we show that f_{Bmin} is proportional to the mass adsorbed at the sensor surface and not influenced by interferences coming from viscoelastic variations of the adsorbed layers or buffers. This parameter was used to study the binding of RXRα to DNA and to calculate the association and dissociation kinetic constants of RXRαDBD-DR1 interaction. We show that RXRαDBD binds to DNA both as a monomer and as a homodimer, and that the mechanism of binding is salt dependent and occurs in two steps. The QCM biosensor data reveals that high ionic strength buffer prevents the unspecific interactions and at lower ionic strength the dissociation of RXRαDBD-DR1 occurs in two phases.

Introduction

Retinoic X receptor α (RXRα) is a transcription factor member of the nuclear hormone receptors that plays an essential role in the regulation of many intracellular receptor signaling pathways. As a transcription factor, RXRα is involved on the gene regulation of different cellular processes., including cellular proliferation, and the metabolism of lipids and xenobiotics[1-7].

RXRα presents a highly conserved DNA-binding domain (DBD), which is very important in the recognition of the DNA response elements. In response to external stimuli, RXRα forms heterodimers with other receptors, including the peroxisome proliferator-activated receptor (PPAR), thyroid receptor (TR), vitamin D receptor (VDR) and retinoic acid receptor (RAR)[1-4]. However, in the presence of 9-cis retinoic acid, RXRα homodimers are formed[5,6] that bind to the RXRα DNA recognition sequence (DR1) which is composed by two direct repeats of AGGTCA polynucleotide sequence separated by one single nucleotide[7].

The mediation in ligand-dependent gene expression makes RXRα transcription factor activity an important topic of study in applied biomedical research. Protein-DNA interactions have been studied with several biophysical techniques, including dynamic light scattering, fluorescence spectroscopy, microcalorimetry, atomic force microscopy (AFM), surface plasmon resonance (SPR) and QCM[8-14]. Among these technologies, QCM has been traditionally applied in label-free microgravimetric applications because the real-time variation of its motional series resonance frequency (Δfs) is proportional to the mass adhered to its surface[15]. Indeed, complex biological processes such as DNA hybridization[16] and protein-DNA interaction can also be monitored and characterized with such acoustic wave biosensors[17]. Nevertheless, QCM application in real-time kinetic studies with biomolecules is limited because changes in the viscoelastic properties of adsorbed films interfere with the Δf_s measurement[18]. Here, we use another mass-dependent frequency variation which is not affected by viscoelastic changes[19]. We demonstrate that the sensor frequency monitored at susceptance spectrum minimum (Δf_{Bmin}) – See ESI Fig. S1 - is an advantageous and effective alternative parameter to the classical Δf_s measurement, and enables a more accurate determination of binding kinetics constants[19].

Another advantage of QCM is the possibility to infer on the mechanical properties of the biological films[11-13,22], which can be explored advantageously to comprehend the underlying biophysical principles of molecular recognition. In particular,

the characterization of the physical properties of anchored DNA sequences has received considerable attention[13,16,23-26].
In this work, we used the QCM with impedance analysis to characterize RXRαDBD interaction with immobilized DNA oligoduplexes. Kinetic binding constants and viscoelastic properties of DNA-protein complex structure were investigated for different salt concentration. We show that the salt dependence of the RXRαDBD-DNA recognition allows the differentiation between specific and nonspecific interaction and calculate the association and dissociation kinetic constants for the RXRα specific and nonspecific interaction with a DNA oligoduplex containing its response element (DR1) and with a random DNA oligoduplex without the DR1 element ($DR1_{neg}$), respectively.

Experimental

RXRαDBD expression and purification

Human RXRαDBD domain (aminoacids 130 to 212 of the full RXR protein) was amplified from the pGEX2TK-hRXRα vector containing the full RXR DNA sequence[27,28] and cloned into the pGEX4T expression vector. *E. coli* BL21-pLysS were transformed with the constructed vector and grown in 2 L LB media. The protein expression was induced with IPTG at 25ºC for 6 hours. The expressed RXRαDBD domain was purified as described elsewhere[5,29]. Briefly, the cells were disrupted by sonication in Tris buffer (20 mM Tris, 150 mM NaCl, pH 8.0) containing 1 mM DTT and 1 mM PMSF. The soluble fraction was collected after centrifugation and loaded to a chromatography column packed with glutathione sepharose 4 fast flow resin (GE Healthcare). The RXRαDBD was eluted with 10 mM of reduced glutathione (GSH) in Tris buffer and stabilized by addition of 10 mM of DTT. High purity (>98%) RXRαDBD protein was further obtained by cation-exchange chromatography[30] using resource S resin (GE Healthcare). The protein was eluted from the column 300 mM NaCl, dialyzed a 4ºC for 24hours against HEPES buffer (20 mM HEPES, 100 mM NaCl, pH 7.5) with 1 mM DTT and 50 µM $ZnCl_2$ and stored at -20ºC. The purification and characterization of RXRαDBD domain is shown in ESI Fig. S2.

Preparation of DNA Oligoduplexes

The specific and nonspecific DNA oligoduplexes sense and antisense primers were purchased from Sigma-Aldrich. The specific DNA sense primer was synthesized with 30 nucleobases including the DR1 response element (underlined) and modified with biotin at the 5' end (5'-[biotin]-GGCGATAGGCAGGTCAAAGGTCACATAGAT-3'). A sense primer with random sequence of 30 nucleobases was used as negative control. In both cases, the sense and antisense strands were annealed by heating to 95ºC during 5 min and cooling to the room temperature in 10 mM Tris pH 8.0 buffer at the concentration of 20 µM. The DNA oligoduplexes were stored at -20ºC until their immobilization at sensor surface.

Preparation of QCM sensors

10 MHz quartz crystals with gold electrodes (0.2 cm^2 of area) were purchased from International Crystal Manufacturing (ICM, USA). The crystals were exposed to UV/ozone (PSDT-UVT, Novascan, USA) for 10 min, immersed into piranha solution (3:1 mixture of sulphuric acid and 30% hydrogen peroxide) for 10 min, rinsed with ultrapure water (18.2 MΩ), and dried under a nitrogen stream. The crystals were then incubated for 24 hours at 4ºC with a mixture of 10% biotin-PEG-dissulfide (LCC Engineering, Switzerland) and 90% 11-hydroxy-1-undecanethiol (Dojindo, Japan) at 1mM in absolute ethanol. The crystals were rinsed with ethanol, water, dried with nitrogen and assembled in a 25 µl acrylic flow cell. A solution of 3 µg/ml of streptavidin (Roche) in PBST, (10 mM Na_2HPO_4, 1.8 mM KH_2PO_4, 2.6 mM KCl, 137 mM NaCl, 0.005% tween-20, pH 7.4) was flow at 100 $\mu l.min^{-1}$ by a high-precision syringe pump (Cetoni, Germany) during 10 minutes. Finally, previously hybridized DNA oligoduplexes at concentration of 0.1 µM was immobilized over the streptavidin layer at the same flow conditions.

Monitoring of the RXRαDBD interactions with the DNA oligoduplexes

A custom-made software for real-time data acquisition from a Network/Impedance/Spectrum Analyzer 4395A (Agilent Technologies) was used to monitor changes in the conductance, G, and susceptance, B, spectra with a 50 kHz frequency span around the QCM resonance as described elsewhere[31,32]. The immobilized DNA oligoduplexes were challenged with different RXRαDBD concentrations (0.05 to 2 µM), using HEPEST (10 mM HEPES, 0.005% tween-20, pH 8.0) containing 10, 200 or 250 mM NaCl as carrier buffer. The flow was maintained at 100 $\mu l.min^{-1}$ and RXRαDBD solutions were applied for 10 min. The biosensor surface was flushed with HEPEST buffer for 25 min. After each cycle of RXRαDBD binding the biosensor surface was regenerated with 0.5 M NaCl in HEPEST buffer during 2 min.

Interaction of GST-RXRDBD with RXRDBD

QCM sensors were activated during 4 h with the cross-linker dithiobis-succinimidyl undecanoate (DSU) followed by 2 h with 1-hydroxy-11-undecanothiol (HUT) in ethanol solutions. Anti-GST antibody was immobilized at 100 $\mu g.ml^{-1}$ during 2 h, and unbounded DSU molecules were inactivated with ethanolamine 1 M. Finally, GST-RXRαDBD was captured by anti-GST and purified RXRαDBD (5 µM) was injected over the sensor surface in HEPEST buffer.

Electrophoretic mobility shift assay

The interactions of RXRαDBD with the specific and unspecific DNA oligoduplexes were promoted in solution for the electrophoretic mobility shift assay (EMSA). 10 nmol mixtures of the tested DNA oliduplexes with RXRαDBD were incubated for 3 hours in the binding buffer (20 mM Tris, 100mM NaCl, 0.005% Tween 20, 10% glycerol, pH 8.0) at room temperature. As controls, the DNA oligoduplexes and the RXRαDBD were incubated in separate solution under the same conditions. The prepared samples were applied in a native acrylamide gel (6%) containing 2.5% glycerol (pre-ran for 1 hour at 100 V at 4ºC). The gel was resolved for 45 min at 90 V and 4ºC using TBE (45 mM Tris, 45 mM boric acid and 1 mM EDTA) as electrophoretic buffer. Finally, the gel was dyed using the silver staining method.

Results and Discussion

A sensor frequency that is not influenced by common interferences

Martin *et al*.[34] demonstrated that at certain conditions, the QCM resonance frequency variation is the sum of the mass load and of the fluids rheological properties contributions ($\Delta f=\Delta f_m+\Delta f_L$). Once the fluid viscosity and density are known, the mass contribution to the resonance frequency variation can be calculated by subtracting the liquid contribution from the measured signal. The Sauerbrey equation[15] can then be applied to quantify the mass variation on the sensor surface. It is known that changes in complex interfacial factors near or at the sensor surface, such as the surface charge, the electrical double layer, and the deposited film viscoelasticity, also affect the propagation of the acoustic wave and, consequently, also contribute to the measured resonance frequency (Δf) signal[18,31,35]. In such cases, complex physical models are used in order to isolate the different contributions to the sensor signal to isolate and estimate the mass contribution[22,26]. Here, we demonstrate that a frequency not affected by these interferences can be directly extracted from the measured admitance spectra, Y=G+iB, where G is the conductance and B is the susceptance. This frequency (Δf_{Bmin}) is the frequency at the minimum of the susceptance spectra, which is also the same at half height of the conductance spectrum (Fig. S1, ESI). The Δf_{Bmin} can be obtained directly from the susceptance or conductance spectra and has been suggested to be only sensitive to mass changes, even in liquid environments[19]. To show this, we use the Butterworth-Van Dyke (BVD) model of the QCM[18], that describes the QCM as an electrical equivalent circuit composed by one resistance (R), one inductance (L), and one capacitance (C) in parallel with one parasitic capacitance (C_0). These parameters are determined from the best fit of the conductance, $G_{BVD}=R/[R^2+(\omega L-1/\omega C)^2]$, and susceptance, $B_{BVD}=\omega C_0-(\omega L-1/\omega C)/[R^2+(\omega L-1/\omega C)^2]$, to the experimental spectra, where $\omega=2\pi f$ is the angular frequency. The values of L and C can be further used to calculate the motional series resonance frequency $f_s = \sqrt{[1/(LC)]} / (2\pi)$ which is the commonly used parameter for the determination of the mass at the surface of the sensor crystal.

Among all the lumped BVD elements, C is related only to the sensor physical material, and it is assumed to be constant upon the mass and liquid loadings, which are known to promote variations of R, L and C_0. In liquid loading the major influencing factors of R and C_0 values are the layer's density and viscosity and the balance of charged species[35], respectively. For the ideal rigid mass loading, which respects the Sauerbrey equation assumptions, $\Delta R\approx 0\ \Omega$ reveling that no dissipation occurs. In such cases the inductance is the only parameter changing, increasing as a result of the deposition of mass. On the other hand, the loading of a viscoelastic material is characterized by a significant variation of R[33-35]. Whenever, capacitive changes occur between the metal electrodes, the C_0 changes. Therefore, we have paid special attention to the variation of R and C_0 in our assays. To demonstrate their importance, all the previously mentioned parameters were extracted during the immobilization of streptavidin onto biotin-functionalized QCM sensors. In the first experiment we have stabilized the QCM in water and injected the streptavidin in PBST. As shown in Fig. 1.A, the sensor's R and C_0 changed upon the injection of the streptavidin. This response was expected since both the charge balance at the surface and the contacting media viscosity are altered after changing from ultrapure water to PBST buffer, affecting both C_0 and R, respectively. As shown in Fig. 1.A, both measured frequencies, f_s and f_{Bmin}, decreased as a result of streptavidin immobilization. Clearly, Δf_{Bmin} is not affected by variations of the buffer properties, as evidenced when switching from streptavidin containing buffer to ultrapure water (Fig. 1.A). On the contrary, an overall increase of Δf_s is observed upon washing with water, stabilizing at a value close to Δf_{Bmin}. These data clearly show that, under these conditions the mass of immobilized streptavidin calculated from Δf_s would be overestimated due to the increase of R and C_0 [35]. This reveals the risk for misinterpretations from the Δf_s signal, as the measured transient recorded when switching from buffer to water can be interpreted as desorption of mass and not as a decrease (or variation) of C_0 and R[35]. Correction factors need to be used to account for the influence of C_0 and R to Δf_s [26], resulting on a transient profile similar to Δf_{Bmin}.

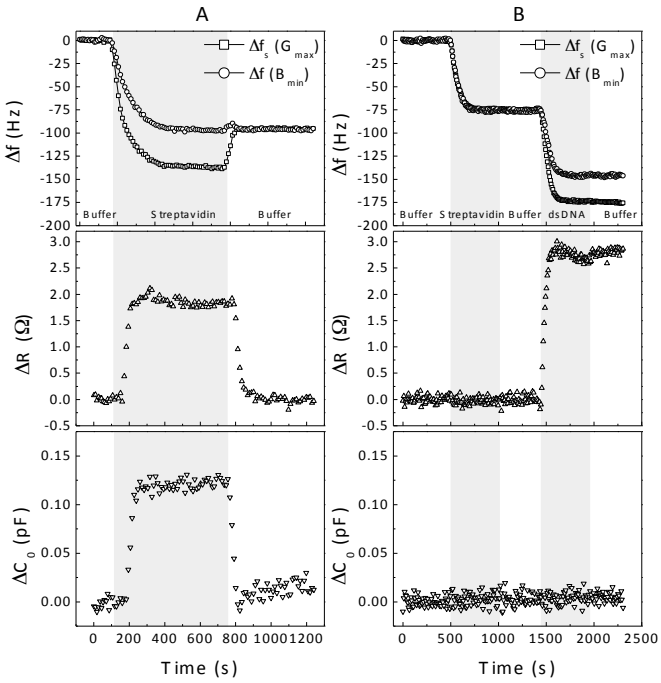

Fig 1. Frequency variations (Δfs and ΔfBmin), resistance variation (ΔR) and capacitance variation (ΔC0) were monitored with (A) and without (B) changes in buffer ionic strength and viscosity. Immobilization of 3 µg/mL streptavidin and 0.1 µM biotinilated dsDNA. Flow injection of 1 mL samples and wash with PBST buffer between injections.

To further demonstrate the influence of R and C_0 on the measured Δf_s, the biotin modified sensors were now stabilized in buffer (instead of water) before switching to the streptavidin in PBST. In this case, the ionic strength and the viscosity of the buffer are maintained (with exception of a minor contribution from the diluted protein) and, as shown in Fig. 1.B, C_0 and R did not change ($\Delta R\approx 0\ \Omega$ and $\Delta C_0\approx 0$ pF). Consequently, the Δf_s and Δf_{Bmin} transients were very similar (Fig 1.B). The total frequency variation (Δf_{Bmin}) during streptavidin immobilization

was 75 Hz, which from the Sauerbrey equation is translated to a streptavidin surface density of 6.5 pmol.cm^{-2}, which is a value very close to previously published data[32]. When immobilizing DNA over the streptavidin layer, different values of Δf_s and Δf_{Bmin} were also measured (Fig. 1B). The immobilization of the DNA oligoduplexes was expected to increase of the viscoelasticity at the sensor surface[36] which was signaled by the QCM biosensor by the increase of R (Fig. 1B). The DNA oligoduplexes viscoelasticity results in a higher dissipation of the acoustic wave energy which explains the 30 Hz difference between Δf_s and Δf_{Bmin} (Fig.1B). Again, it is clear that the Δf_s cannot be directly used to estimate any mass-related quantities, as it would lead to overestimations and to erroneous conclusions when studying viscoelastic mass loadings. The total mass estimated for the immobilized DR1 DNA oligoduplexes from the Sauerbrey equation applied to Δf_{Bmin} is 3.3 pmol, which corresponds to 5.3×10^{10} immobilized DR1 molecules and to a 1:2.5 ratio to streptavidin molecules. It is known that, due to stereochemical effects and negative cooperativity, the streptavidin cannot interact with more than 2 to 3 of its 4 biotin binding sites[32]. Thus, the 1:2.5 ratio obtained from the mass estimations with Δf_{Bmin} is actually very close to what was expected considering a full monolayer of DR1 over a streptavidin film[32].

Acoustic detection of RXRαDBD interaction with DNA

The interaction of RXRαDBD in HEPEST buffer with 150 mM NaCl with immobilized DR1 and nonspecific DNA oligoduplexes was followed by monitoring the variations of the biosensor's f_{Bmin} and R. The data collected during the RXRαDBD's binding, washing and desorption from the modified QCM surface is represented in Fig. 2. We show that, under such conditions, the RXRαDBD binds similarly to both the specific DR1 (Fig. 2.A) and unspecific DR1$_{neg}$ (Fig. 2.B) DNA oligoduplexes, leading to identical frequency variations. These data clearly depict the difficulty to distinguish the association phases of RXRαDBD to the immobilized specific and unspecific DNA oligoduplexes, which is inherent to the TF surface charge and to the TF's mechanism of DNA recognition. Considering the isoelectric point of RXRαDBD (pI = 9.5), the protein is mostly positively charged under the experimental conditions, and thus it is likely to establish electrostatic interactions with the negatively charged DNA films despite their oligonucleotide sequence. Furthermore, the recognition and association of transcription factors to DNA is known to follow a two step mechanism in which long range and unspecific electrostatic interactions occur initially to attract the TF close to the DNA sequences and is then followed by the establishment of short-range and specific van der Walls interaction and hydrogen bonding[37-39]. Since frequency variation measurements are related with the mass at the sensor surface, it was not expectable that the measurement of the Δf_{Bmin} would by itself distinguish the two steps of the RXRαDBD binding to the immobilized oligoduplexes. Nevertheless, despite the similar frequency variation transients measured during the association phase for both specific and non specific DNA sequences, the dissociation phases were very discernible – Fig. 2. As shown, when RXRαDBD interacts specifically with DR1 (Fig. 2.A), the complex was more stable leading to a slower dissociation phase as compared with the interaction with the non-specific DR1$_{neg}$ (Fig. 2.B). Indeed, washing the sensor with the HEPEST buffer was found to be sufficient for a fast and complete removal of the RXRαDBD from the biosensor's surface modified with the DR1$_{neg}$ DNA oligoduplex, in which case the sensor regeneration was achieved in less than 15 min as signaled by the restoring of the initial frequency value – Fig. 2.B. On the contrary, the complete desorption and wash-out of RXRαDBD from the sensor modified with the specific DR1 DNA oligoduplex could only be achieved by increasing the buffer salt concentration to 0.5 M (Fig. 2.A). This salt-driven regeneration was found to be very reproducible and useful to perform the kinetic study of RXRαDBD while maintaining intact the biosensor basal structure of immobilized DNA oligoduplexes via streptavidin-biotin affinity coupling. Indeed, the interaction of streptavidin-biotin is very strong and stable having a long half-life, $t_{1/2} \approx 3$ days[40], which makes this biosensor activation and regeneration methods very robust for relatively fast kinetic studies.

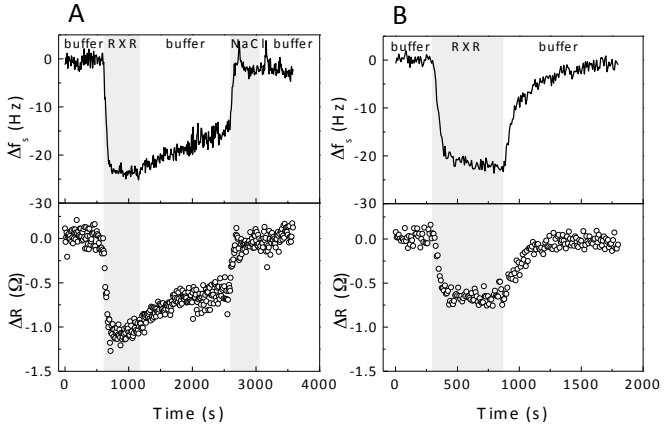

Fig. 2. Kinetic plots of the changes in frequency (lines) and motional resistance (open circles) due the interaction of 0.25 μM RXRDBD with immobilized DR1 (A) and non-specific DNA (B) at presence of HEPEST buffer with 150 mM NaCl.

Considering our measured data in combinations with the currently accepted mechanism of TF recognition and binding to DNA[37,39,41,42], we hypothesized that the key to kinetically distinguish the specific from unspecific complex formation of TFs with DNA oligoduplexes rely on the effect of the concentration of salt. A set of experiments were carried out with HEPEST buffer containing 100, 150 and 250 mM of NaCl to verify the effect of buffer's ionic strength over the kinetics of formation of RXRαDBD-DNA complexes - Fig. 3. A one-to-one binding model[31] was used to estimate the binding rates of RXRαDBD to immobilized DNA. The time dependency of the sensor surface coverage is described $\theta = C\times\theta_\infty/(C+k_d/k_a) \times [1 -$

$e^{-t/\tau}$] , where θ_∞ is the total available DNA binding sites at the sensor surface and C is the concentration of RXRαDBD in solution, $\tau = [k_a \times C + k_d]^{-1}$ is the relaxation time of binding, and k_a and k_d are the association and dissociation rate constants. According to this 1:1 binding model the dissociation of RXRαDBD from the DNA oligoduplexes follows an exponential decay given by $\theta = \theta_0 \times e^{-kd \times t}$, where θ_0 represented the surface coverage by RXRαDBD-DNA complexes at the beginning of the dissociation process. The dissociation rate constant, k_d, is directly calculated from the fitting of this equation to experimental dissociation data.

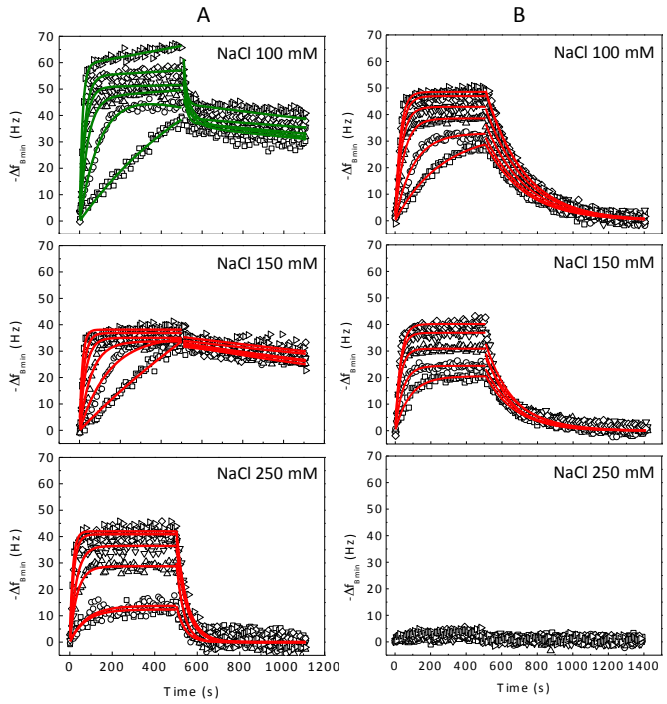

Fig 3. Kinetic transients of RXRDBD: interactions in presence of 100 (top panel), 150 (middle panel) and 250 mM of NaCl (bottom panel) with specific DNA oligoduplex DR1 (A) and non-specific DNA oligoduplex DR1neg (B). Increasing concentrations of protein (□-0.05, ○-0.1, △-0.25, ▽-0.5, ◇-1.0 and ▷-2.0 μM) were injected over the same DNA surface after regeneration. Each transient is the average of three experiments. Solid lines represent the fit of a 1:1 (red) and 2:1 (green) binding model to the experimental data points during the association and dissociation phases.

As shown in Fig. 3 the salt has an important effect in the formation and stability of protein-DNA complexes. While the 1:1 model fitted well to the experimental data at 150 mM and 250 mM NaCl, this was not observed for 100 mM NaCl (Fig.3A). The dissociation phase for 100 mM Nacl (Fig. 4) clearly show two stages and the residuals of the fit to a single exponential decay are not randomly dispersed (Fig. 4A).

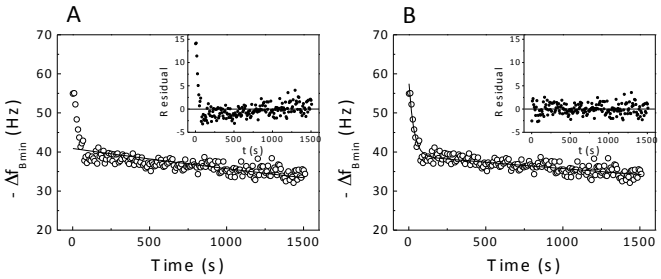

Fig. 4. Dissociation transient between 1μM of RXRαDBD specific complex with DR1 DNA oligoduplex at 100 mM NaCl. Minimum squared error nonlinear fittings were used to adjust experimental data to 1:1 interaction model (A) and for the double exponential model (B). The insets show the residual from the model fit.

As such, we tested a double exponential decay, $\theta = \theta_1 \times e^{-(kd1 \times t)} + \theta_2 \times e^{-(kd2 \times t)}$ to describe the dissociation of RXRαDBD for the 100 mM NaCl. The double exponential decay model resulted in a clear improvement of the fitting, as shown by the random dispersion of the residuals (Fig. 4B). These data reveals the dissociation in two steps in accordance with previous reports for other nuclear receptors[43]. Two dissociation rate constants, k_{d1} and k_{d2} were thus determined for the RXRαDBD-DNA interaction at 100 mM NaCl – Table 1

Table 1. Kinetic parameters for interaction RXRDBD:DR1

NaCl (mM)	DNA Oligoduplex	k_a ($\times 10^{-4}$ $M^{-1}s^{-1}$)	k_d ($\times 10^{4}$ s^{-1})	K_D (nM)
100	DR1(†)	3.2 ± 0.4	380 ± 61	1180±240
	DR1(‡)	3.7 ± 0.7	1.2 ± 0.2	3.2 ± 0.8
	$DR1_{neg}$	3.0 ± 0.6	9.6 ± 1.2	31 ± 7.3
150	DR1	3.2 ± 0.4	3.2 ± 0.6	9.9 ± 2.0
	$DR1_{neg}$	2.4 ± 0.2	61 ± 5.5	252 ± 31
250	DR1	2.9 ± 0.5	227 ± 62	768 ± 250
	$DR1_{neg}$	n.d.	n.d.	n.d.

† Interaction of with DR1 DNA oligoduplex in the monomer form;
‡ Interaction of with DR1 DNA oligoduplex in the dimer form;
n.d. Not detected, without interaction.

RXRαDBD Homodimerization

As it was previously suggested that RXRαDBD interacts with the motif DR1 in the homodimer form, the results in Fig. 4 suggest that the two exponential decays reflect the dissociation of the monomer and of the dimer forms from DNA. In order to prove that RXRαDBD can for homodimers in solution under these experimental conditions, we generated a biosensor with immobilized RXRαDBD and studied the kinetics of homodimer formation. To do so, a fusion protein of GST-RXRαDBD was immobilized at the sensor surface under controlled surface orientation using a previously immobilized anti-GST antibody and was challenged with purified RXRαDBD. The protein-protein interaction resulted in the formation of a rigid complex,

with no variation of the sensor motional resistance, with a kinetic profile following a simple 1:1 interaction model (Fig. 5.A). The control of RXRαDBD interaction with immobilized anti-GST did not show significant adsorption (<10%), which reveals the specificity of the homodimerization interaction on the sensor. This experiment confirms the possibility of co-existence of the RXRαDBD monomer and dimer forms in solution. The rate constants were calculated from the fit of the 1:1 model for the association and desorption phases in Fig. 5.A, enabling the calculation of the equilibrium constant $K_D = k_d/k_a = 8.5x10^{-7}$ M which characterizes the homodimerization interaction of RXRαDBD.

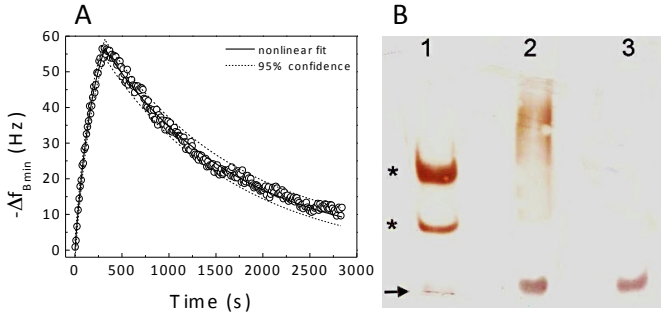

Fig. 5. Homodimerization of RXRαDBD. (A) sensor data Δf_{Bmin} corresponding to the association and dissociation phases of the dimerization interaction of free and immobilized RXRαDBD. The non-linear fit to a one-to-one interaction model is shown (solid line) together with the 95% confidence interval (dashed lines). (B) Electrophoretic mobility shift assay of the RXRαDBD complexes with DR1 (lane 1) and $DR1_{neg}$ (lane 2). Lane 3 correspond to a control with just DR1 DNA oligoduplex. Protein-DNA complexes and free DNA oligoduplexes are indicated with "*" and "→", respectively

The homodimerization of RXRαDBD and the interaction of this nuclear receptor with DNA both as a monomer and an homodimer was further demonstrated by an electrophoretic mobility shift assay (Fig. 5.B). In the presence of the oligoduplex containing the specific binding sequence (DR1) two protein bands are visible corresponding to two DNA-protein complexes – lane 1, Fig. 5.B. The migration path of these protein bands reveals a two-fold relationship on the size (weigh) of the proteins, being thus an evidence of RXRαDBD homodimerization. Figure 5.B also show that when unspecific oligoduplexes were present, only a dragging of protein was observed (no clear protein bands) and no protein migration was observed in the absence of any DNA sequence.

It is thus evident that under these experimental conditions RXRαDBD interacts with immobilized DR1 oligoduplexes simultaneously as a monomer (A) and as a dimer (A_2).

Mechanism of RXRαDBD interaction with immobilized DNA oligoduplexes

A binding mechanism of two species to the same immobilized receptor would better describe the experimental data[43] – See ESI. This model was used to describe the interaction of RXRαDBD simultaneously as a monomer (A) and a dimer (A_2) with immobilized DNA (B), and the association rate constants, k_{a1} and k_{a2} were calculated through non linear fitting to the adsorption phase in Fig. 3A – Details in the ESI.

The kinetic constant values for the different salt concentrations are summarized in Table 1. The ionic strength has no significant influence on the association rate constants, k_a, both for the interaction of RXRαDBD with the DR1 or $DR1_{neg}$ DNA oligoduplexes. On the other hand, the dissociation rate constant (k_d) of RXRαDBD-DR1 complexes increase with the increase of the concentration of salt, which consequently is similarly reflected on the equilibrium constant (K_D). For all the cases, the unspecific interaction shows higher k_d values. Furthermore, at 250 mM NaCl no significant binding was measured for RXRαDBD to $DR1_{neg}$ DNA oligoduplex. These data reveals that the binding of RXRαDBD to DNA is drastically reduced at higher ionic strength, as also reported for other transcription factors[44]. Our data suggests that this decrease of the RXRαDBD peptide ability to bind is not associated with alteration of its affinity, as these would be reflected by changes of the association rate constant. In fact, as increasing k_d values were calculated for increasing salt concentrations, we hypothesize that such decrease of the RXRαDBD peptide ability to bind is associated to electrostatic shielding effects of the positive charges of RXRαDBD by the salt. This result adds to the hypothesis of a two-step binding mechanism in which the first step is driven by electrostatic interactions whilst the second step is driven by affinity interactions[44-47].

Conclusions

We have shown that the QCM is an efficient tool to characterize protein-DNA complexes. In particular the sensor can detect the binding of the transcription factor RXRαDBD to its specific recognition DNA sequence DR1. A sensor frequency variation that is only dependent on the variation of the mass, therefore being tolerant to changes of viscoelasticity changes on the adsorbed layer, was identified and used successfully to calculate the association and dissociation kinetic constants of RXRαDBD-DR1 interaction. We show that high ionic strength buffer prevents unspecific interactions and at lower ionic strength the dissociation of RXRαDBD-DR1 occurs in two phases.

Kinetic studies of TF-DNA binding enables both the identify of DNA binding sites (RE), which is one of the major goals of TF research in general, and the quantification of the affinity of the TF-DNA. As shown, the methodology herein developed, is an important tool in understanding and quantifying the mechanism of such interaction.

Acknowledgements

The authors thank P. Lefebvre (INSERM, Lille) for providing the expression vector pGEX2TK-hRXRα.
This work was supported by FCT - Fundação para a Ciência e a Tecnologia, project ref. PEst-OE/EQB/LA0023/2013. The authors acknowledge Fundação para a Ciência e a Tecnologia (FCT) the financial support through the projects PEst-OE/EQB/LA0023/2013, PTDC/EBB-EBI/108517/2008 and PTDC/SAU-BEB/105189/2008, and the PhD grants SFRH/BD/33720/2009 and SFRH/BD/38136/2007.

Notes and references

[a]IBB-Institute for Biotechnology and Bioengineering, Centro de Biomedicina Molecular e Estrutural, Universidade do Algarve, 8005-139 Faro, Portugal;
[b] Corresponding author E-mail: gferrei@ualg.pt;
† Electronic Supplementary Information (ESI) available: Electrical characterization of the QCM; Purification of RXRaDBD; and two analyte binding model. See DOI: 10.1039/b000000x/

1. D. J. Mangelsdorf and R. M. Evans, *Cell*, 1995, **83**, 841–850.
2. P. Lefebvre, Y. Benomar and B. Staels, *Trends Endocrinol. Metab.*, 2010, **21**, 676–683.
3. L. N. Wei, *Annu. Rev. Pharmacol. Toxicol.*, 2003, **43**, 47–72.
4. C. Zechel, X. Q. Shen, J. Y. Chen, Z. P. Chen, P. Chambon and H. Gronemeyer, *EMBO J.*, 1994, **13**, 1425–1433.
5. D. M. Heery, B. Pierrat, H. Gronemeyer, P. Chambon and R. Losson, *Nucleic Acids Res.*, 1994, **22**, 726–731.
6. A. IJpenberg, N. S. Tan, L. Gelman, S. Kersten, J. Seydoux, J. Xu, D. Metzger, L. Canaple, P. Chambon, W. Wahli and B. Desvergne, The *EMBO J.*, 2004, **23**, 2083–2091.
7. F. Rastinejad, T. Perlmann, R. M. Evans and P: B. Sigler, *Nature*, 1995, **375**, 203–211.
8. U. Błaszczyk, A. Polit, A. Guz, and Z. Wasylewski, *J. Protein Chem.*, 2001, **20**, 601–610.
9. R. Favicchio, A. I. Dragan, G. G. Kneale and C. M. Read, in *DNA-Protein Interactions: Methods in Molecular Biology*, ed. T. Moss and B. Leblanc, Humana Press, 3rd edn, 2009, vol. 543, ch. 35, pp. 589–611.
10. J. Xu, K-W. Liu, K. S. Matthews and S. L. Biswal, *Langmuir*, 2011, **27**, 4900–4905.
11. Lane, A. N.; Kelly, G.; Ramos, A.; Frenkiel, T. A. Determining binding sites in protein–nucleic acid complexes by cross-saturation. *J. Biomol. NMR*, 2001, **21**, 127–139.
12. M. Lysetska, A. Knoll, D. Boehringer, T. Hey, G. Krauss and G. Krausch, *Nucleic Acids Res.*, 2002, **30**, 2686–2691.
13. G. Papadakis, A. Tsortos , K. Mitsakakis and E. Gizeli, *FEBS lett.*, 2010, **584**, 935–940.
14. W. Y. X. Peh, E. Reimhult, H. F. Teh, J. S. Thomsen and X. Su, *Biophys. J.*, 2007, **92**, 4415–4423.
15. G. Sauerbrey, *Z. Physik*, 1959, **155**, 206–222.
16. X. Su, Y-J. Wu, R. Robelek and W. Knoll, *Langmuir*, 2005, **21**, 348–353.
17. X. Su, R. Robelek, Y. Wu, G. Wang and W. Knoll, *Anal. Chem.*, 2004, **76**, 489–494.
18. G. N. M. Ferreira, A-C. da-Silva and B. Tomé, *Trends Biotechnol.*, 2009, **27**, 689–697.
19. A. Itoh and M. Ichihashi, *Meas. Sci. Technol.,* 2008, **19**, 075205.
20. D. Johannsmann, *Phys. Chem. Chem. Phys.*, 2008, **10**, 4516–4534.
21. Y. Jiménez, R. Fernández, R. Torres and A. Arnau, *IEEE Trans. Ultrason., Ferroelectr., Freq. Control*, 2006, **53**, 1057–1072.
22. J. de-Carvalho, R. M. M. Rodrigues, B. Tomé, S. F. Henriques, N. P. Mira, I. Sá-Correia, G. N. M. Ferreira, *Analyst*, 2014, DOI: 10.1039/C3AN01682J.
23. W. Tang, D. Wang, Y. Xu, N. Li and F. Liu, *Chem. Commun.*, 2012, **48**, 6678–6680.
24. G. C. DeNolf, L. Haack, J. Holubka, A. Straccia, K. Blohowiak, C. Broadbent and K. R. Shull, *Langmuir*, 2011, **27**, 9873–9879.
25. A. Tsortos, G. Papadakis, K. Mitsakakis, K. A. Melzak and E. Gizeli, *Biophys. J.*, 2008, **94**, 2706–2715.
26. H. Su and M. Thompson, *Can. J. Chem.*, 1996, **74**, 344–358.
27. B. Lefebvre, Y. Benomar, A. Guédin, A. Langlois, N. Hennuyer, J. Dumont, E. Bouchaert, C. Dacquet, L. Pénicaud, L. Casteilla, F. Pattou, A. Ktorza, B. Staels and P. Lefebvre, *J. Clin. Invest.*, 2010, **120**, 1454–1468.
28. B. Lefebvre, C. Brand, P. Lefebvre and K. Ozato, *Mol. Cell. Biol.*, 2002, **22**, 1446–1459.
29. Q. Zhao, S. Khorasanizadeh, Y. Miyoshi, M. A. Lazar and F. Rastinejad, *Mol. cell*, 1998, **1**, 849–861.
30. S. M. A. Holmbeck, M. P. Foster, D. R. Casimiro, D. S. Sem, H. J. Dyson and P. E. Wright, *J. Mol. Biol.*, 1998, **281**, 271–284.
31. J. M. Encarnação, L. Rosa, R. Rodrigues, L. Pedro, F. A. da-Silva, J. Gonçalves and G. N. M. Ferreira, *J. Biotechnol.*, 2007, **132**, 142–148.
32. J. M. Encarnação, R. Baltazar, P. Stallinga and G. N. M. Ferreira, *J. Mol. Recognit.*, 2008, **22**, 129–137.
33. G. N. M Ferreira, J. M. Encarnação, L. Rosa, R. Rodrigues, R. Breyner, S. Barrento, L. Pedro, F. A. da-Silva and J. Gonçalves, *Biosens. Bioelectron.,* 2007, **23**, 384–392.
34. S. J. Martin, V. E. Granstaff and G. C. Frye, *Anal. Chem.*, 1991, **63**, 2272–2281.
35. J. M. Encarnação, P. Stallinga and G. N. M. Ferreira, *Biosens. Bioelectron.*, 2007, **22**, 1351–1358.
36. C. Larsson, M. Rodahl and F. Hook, *Anal. Chem.*, 2003, **75**, 5080-5087.
37. A. B. Kolomeisky, *Phys. Chem. Chem. Phys.*, 2011, **13**, 2088–2095.
38. H-X Zhou, *PNAS*, 2011, **108**, 8651–8656.
39. A. Marcovitz and Y. Levy, *PNAS*, 2011, **108**, 17957–17962.
40. N. M. Green, in Avidin-Biotin Technology: Methods in Enzymology, ed. M. Wilchek and E. A. Bayer, Elsevier, 1990, vol. 184, ch. 5, 51–67.
41. M. A. D. de-la-Rosa, E. F. Koslover, P. J. Mulligan and A. J. Spakowitz, Biophysical journal, 2010, **98**, 2943–2953.
42. A. Marcovitz and Y. Levy, *Biophys. J.*, 2013, **104**, 2042–2050.
43. B. Cheskis and L. P. Freedman, *Biochemistry*, 1996, **35**, 3309–3318.
44. D. J. Hart, R. E. Speight, M. A. Cooper, J. D. Sutherland and J. M. Blackburn, *Nucleic Acids Res.*, 1999, **27**, 1063–1069.
45. Q. Zhao, S. A. Chasse, S. D. M. L. Sierk, B. Ahvazi and F. Rastinejad, *J. Mol. Biol.*, 2000, **296**, 509–520.
46. P. L. DeHaseth, T. M. Lohman, M. T. Record Jr., *Biochemistry*, 1977, **16**, 4783–4790.
47. P. L. Privalov, A. I. Dragan and C. Crane-Robinson, *Nucleic Acids Res.*, 2011, **39**, 2483–2491.